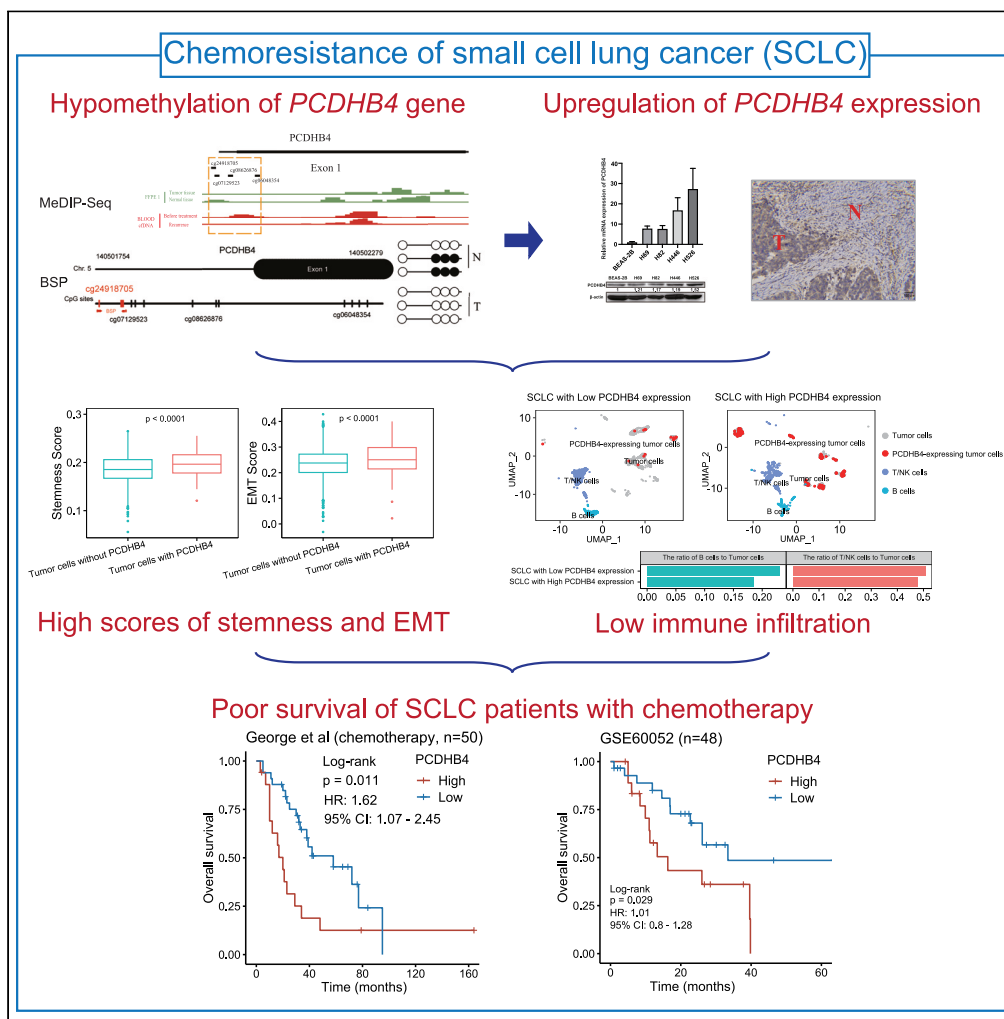


Article

Cisplatin resistance-related transcriptome and methylome integration identifies *PCDHB4* as a novel prognostic biomarker in small cell lung cancer



Qizhi Zhu, Meng Fu, Jian Qi, ..., Jinfu Nie, Bo Hong, Weiping Xu

bhong@hmfli.ac.cn (B.H.)
weipingx@ustc.edu.cn (W.X.)

Highlights

High expression of *PCDHB4* is associated with poor survival of SCLC

PCDHB4 gene is hypomethylated and upregulated in SCLC

PCDHB4 promotes SCLC proliferation and chemoresistance

High *PCDHB4* expression is associated with low immune infiltration, stemness, and EMT



Article

Cisplatin resistance-related transcriptome and methylome integration identifies *PCDHB4* as a novel prognostic biomarker in small cell lung cancer

Qizhi Zhu,^{1,2} Meng Fu,^{1,2,3} Jian Qi,^{1,2,3} Ziming Xu,² Yongguang Wang,³ Zhipeng Wang,^{1,2,3} Dan Wang,² Jiajia Liu,² Ruiping Du,³ Xin Wei,^{1,2} Hongzhi Wang,^{1,3} Jinfu Nie,^{1,3} Bo Hong,^{1,3,5,*} and Weiping Xu^{1,2,4,*}

SUMMARY

Platinum-based chemo-resistance is the major issue for the treatment of small cell lung cancer (SCLC). The integrative analysis of multi-omics data is a reliable approach for discovering novel biomarkers associated with chemo-resistance. Here, multi-omics integrative analysis and Cox regression found that higher expression of *PCDHB4* was associated with poorer survival of SCLC patients who received chemotherapy. *PCDHB4* gene was hypomethylated and upregulated in SCLC, which was validated in the levels of promoter methylation, mRNA, and protein expression. Mechanistically, using bulk RNA-seq data, functional enrichment analysis indicated that higher *PCDHB4* expression was associated with lower immune infiltration. The analysis of single-cell RNA-seq (scRNA-seq) found that SCLC cells with *PCDHB4* expression exhibited the characteristics of stemness and EMT. In addition, the high expression and hypomethylation of *PCDHB4* were also significantly associated with poor survival in lung squamous cell carcinoma. In summary, *PCDHB4* is a potential prognostic biomarker of platinum-based chemotherapy in SCLC.

INTRODUCTION

Small cell lung cancer (SCLC) is a very aggressive neuroendocrine tumor. Platinum-based chemotherapy (cisplatin or carboplatin) is the standard treatment for SCLC. The response of SCLC patients to chemotherapy is variable.^{1,2} The prediction of therapeutic response and prognosis is still difficult, so it is necessary to develop new prognostic biomarkers in SCLC.

Recently, comprehensive bioinformatics analyses have been used to classify patients and identify biomarkers to predict therapeutic response and prognosis in SCLC.³ By analyzing RNA-seq data of SCLC tumors, a study classified SCLC into 4 subtypes: SCLC-A, SCLC-N, SCLC-P, and SCLC-I.⁴ When applying the 4 subtypes into the IMpower133 clinical trial, the SCLC-P subtype was found to have the worst prognosis in the carboplatin/etoposide treatment group.⁵ Via single-cell RNA-seq (scRNA-seq) of circulating tumor cell-derived xenografts (CDX), Stewart et al. revealed that intratumoral heterogeneity was increased after the onset of chemo-resistance in SCLC.⁶ A scRNA-seq study found that an SCLC subpopulation with high *PLCG2* expression was associated with stem-like and pro-metastatic features, as well as worse overall survival (OS).⁷ RNA-seq of SCLC patient-derived xenografts (PDX) identified *SLFN11*, whose expression was decreased in chemo-resistant SCLC.⁸

The identification of abnormal DNA methylation in human cancer is expected to discover new diagnostic markers that are more stable than RNA samples.⁹ Increasing evidence has demonstrated that DNA methylation plays an important role in SCLC development and drug resistance. A microarray study of CpG methylation identified SCLC-specific DNA methylation sites in neural cell fate-specifying transcription factor genes (*NEUROD1*, *HAND1*, *ZNF423*, and *REST*). The methylation of these genes could result in a differentiation defect of neuroendocrine cells, thus promoting the transition toward SCLC.¹⁰ An integrated study of DNA methylation array and drug sensitivity in SCLC cell lines identified the increased promoter methylation of *SLFN11* that correlated with resistance to DNA damaging agents.¹¹

Aberrant DNA methylation is associated with abnormal gene expression. However, the integrated analysis of DNA methylation and gene expression in SCLC has not been studied thus far. In this study, by performing a comprehensive data analysis of gene expression, DNA methylation, drug sensitivity, and patient survival, we identified the *PCDHB4* gene, and its expression and CpG methylation were validated as novel prognostic biomarkers in SCLC, as well as the other subtype of lung cancer, lung squamous cell carcinoma (LUSC).

¹Hefei Institutes of Physical Science, Chinese Academy of Sciences, Hefei, Anhui, P.R. China

²University of Science and Technology of China, Hefei, Anhui, P.R. China

³Hefei Cancer Hospital of CAS, Institute of Health and Medical Technology, Hefei Institutes of Physical Science, Chinese Academy of Sciences, Hefei, Anhui, P.R. China

⁴Department of Geriatrics, Gerontology Institute of Anhui Province, The First Affiliated Hospital of USTC, Division of Life Sciences and Medicine, University of Science and Technology of China, Hefei, Anhui, P.R. China

⁵Lead contact

*Correspondence: bhong@hmfl.ac.cn (B.H.), weipingx@ustc.edu.cn (W.X.)

<https://doi.org/10.1016/j.isci.2024.110413>



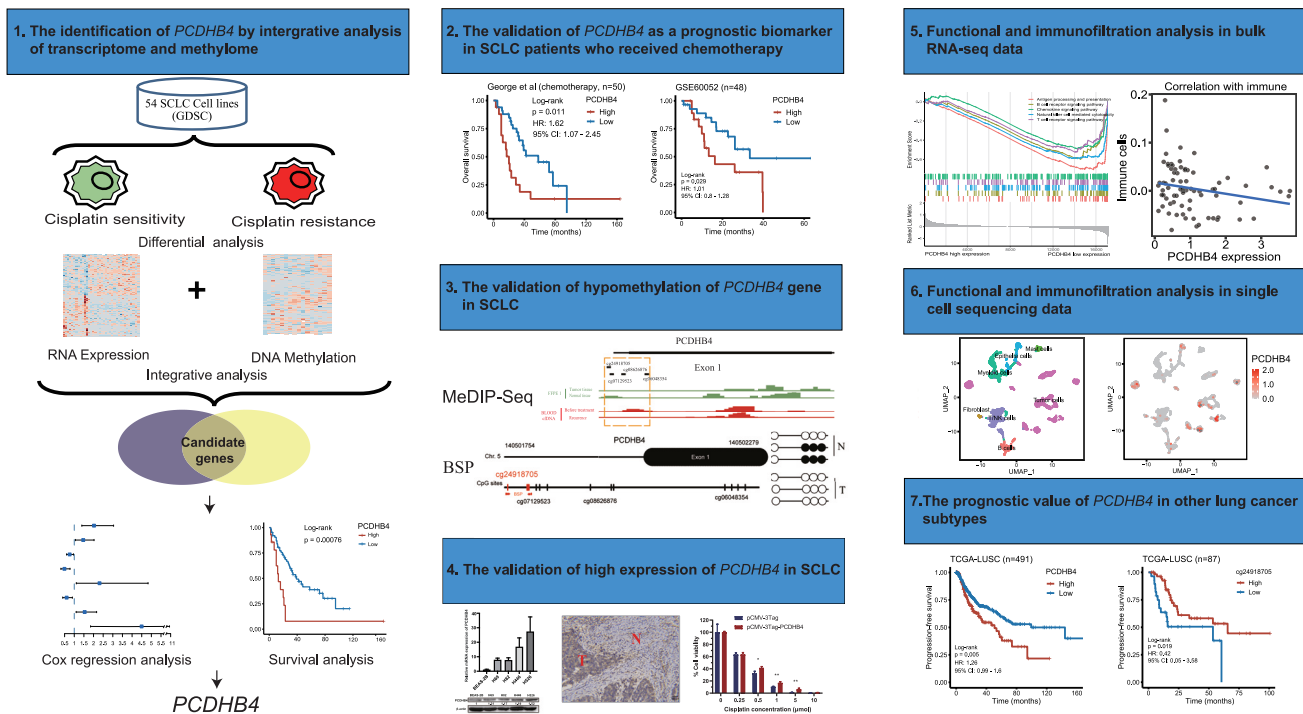


Figure 1. The workflow of the study

RESULTS

Identification of cisplatin resistance-associated genes that may be mediated by DNA methylation in small cell lung cancer cells

The workflow of the study is shown in Figure 1. To identify cisplatin resistance-associated genes that may be regulated by DNA methylation, we first collected gene expression data and cisplatin IC50 values in 54 SCLC cell lines from GDSC. SCLC cell lines were divided into 13 cisplatin-sensitive cell lines (IC50 < 10) and 41 cisplatin-resistant cell lines (IC50 > 10) (Figure 2A; Table S1). We mined differentially expressed genes between cisplatin-sensitive and cisplatin-resistant SCLC cells. According to the cut-off of $p < 0.05$ and $|\log FC| \geq 0.5$, 316 differentially expressed genes were identified, including 185 up-regulated genes and 131 down-regulated genes (Figures 2A and 2B). We then collected DNA methylation data in SCLC cell lines from GDSC and analyzed the differentially methylated sites between cisplatin-sensitive and cisplatin-resistant SCLC cells. According to the cut-off of $p < 0.05$ and $|\log FC| \geq 0.1$, a total of 4833 differentially methylated CpG sites were detected, of which 2442 sites were hypermethylated and 2391 were hypomethylated (Figures 2A and 2C). The 4833 differential CpG sites were located in different regions of genes, including the first exon (5.7%), 3' UTR (3.7%), 5' UTR (12.9%), gene body (45.1%), TSS1500 (21.6%) and TSS200 (11%) (Figure 2D). Generally, the hypermethylation and hypomethylation of the promoter in a gene correspond to its low and high expression, respectively. We intersected the down-regulated/hypermethylated genes as well as the up-regulated/hypomethylated genes. The Venn diagram identified 62 genes, including 18 down-regulated/hypermethylated genes and 44 up-regulated/hypomethylated genes (Figure 2A; Table S2). GO analysis revealed that the top 10 terms of the 316 differentially expressed genes were enriched in extracellular organization and cell-cell junction (Figure 2E). In summary, we identified 62 cisplatin resistance-associated genes whose expression may be regulated by DNA methylation in SCLC cells.

Identification of the *PCDHB4* gene, whose high expression is associated with poor prognosis in small cell lung cancer patients

Since chemo-resistance is related to poor prognosis, we further applied Cox regression analysis to identify the genes associated with the survival of SCLC patients. We used a previously published dataset that included the RNA-seq and survival data of 77 SCLC patients.¹² Using the 62 cisplatin resistance-associated genes, univariate Cox regression analysis identified 8 genes (*SLMO2*, *SGCE*, *SCRN1*, *HDAC7*, *KIAA1826*, *ITPR1L2*, *PCDHB4*, and *HSPB3*), and their expression was significantly associated with the OS in SCLC patients (Figure 3A). Furthermore, multivariate Cox regression analysis indicated that the expression of the *HDAC7*, *PCDHB4*, or *HSPB3* gene was an independent prognostic factor in SCLC patients (Figure 3B). Kaplan-Meier analysis showed that high expression of the *PCDHB4* or *HSPB3* gene was significantly associated with poor OS in SCLC patients, while low expression of the *HDAC7* gene was significantly associated with poor OS in SCLC patients (Figure 3C).

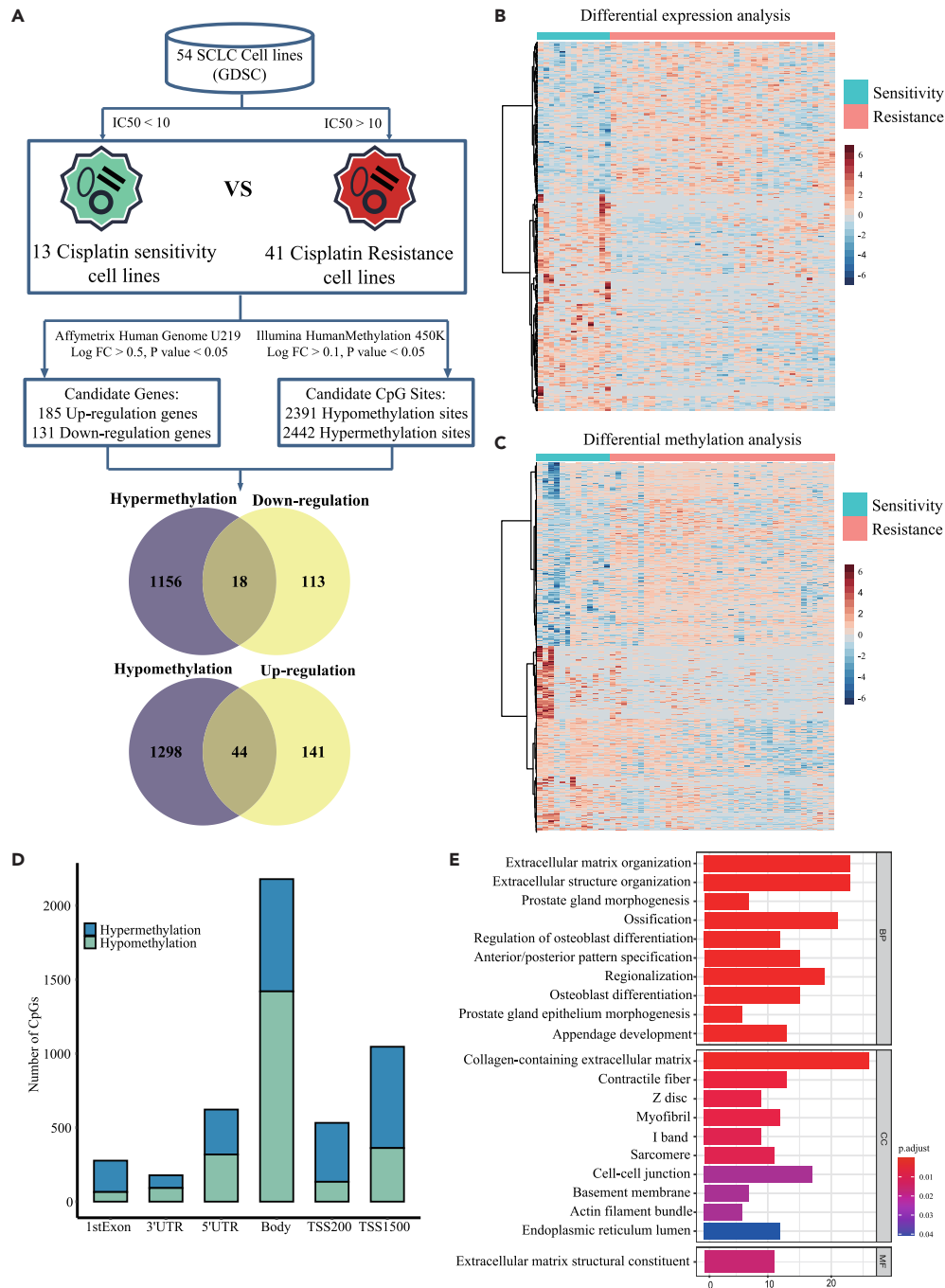


Figure 2. Integrative analysis of differential DNA methylation and gene expression between cisplatin-sensitive and cisplatin-resistant SCLC cell lines (A) The workflow of bioinformatics analysis. The integrative analysis identifies 18 down-regulated/hypermethylated genes and 44 up-regulated/hypomethylated genes.

(B) Heatmap of the differentially expressed genes between cisplatin-sensitive and cisplatin-resistant SCLC cell lines.

(C) Heatmap of the differentially methylated CpG sites between cisplatin-sensitive and cisplatin-resistant SCLC cell lines.

(D) The distribution of the differentially methylated CpG sites across gene regions.

(E) GO analysis of the differentially expressed genes (top 10 terms).

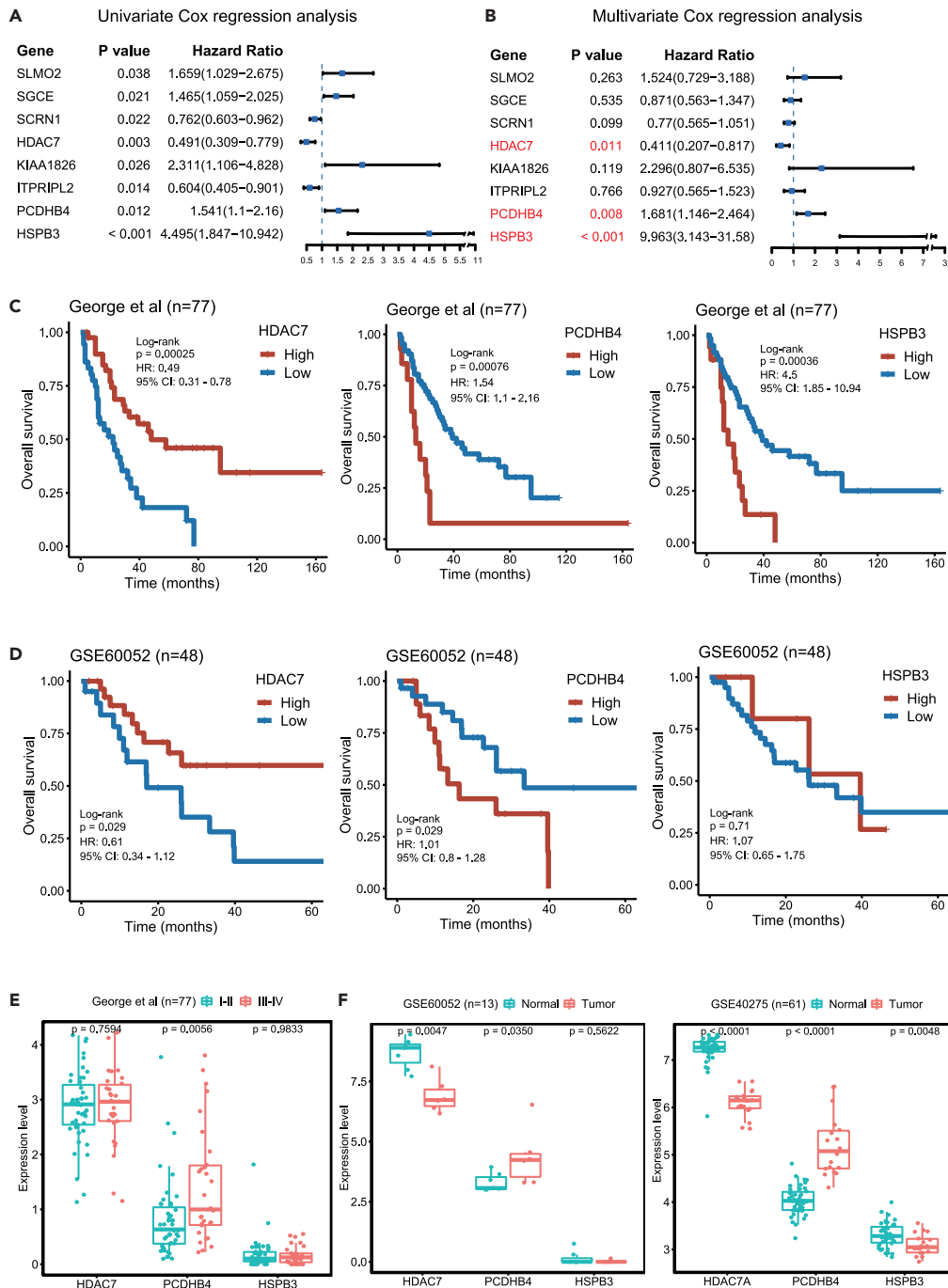


Figure 3. The *PCDHB4* gene is associated with SCLC prognosis

(A) Univariate Cox regression identifies 8 genes associated with the OS of SCLC patients.

(B) Multivariate Cox regression identifies 3 independent prognostic genes (*HDAC7*, *PCDHB4*, and *HSPB3*).

(C) Kaplan-Meier curves in 77 SCLC patients based on the expression of *HDAC7*, *PCDHB4*, or *HSPB3* using the George dataset.

(D) Kaplan-Meier curves in 48 SCLC patients based on the expression of *HDAC7*, *PCDHB4*, or *HSPB3* using an independent validation dataset GEO: GSE60052.

(E) Boxplot showing the expression of *HDAC7*, *PCDHB4*, and *HSPB3* in different stages of SCLC. The differences between groups were analyzed by Wilcoxon test and $p < 0.05$ was considered statistically significant.

(F) Boxplot showing the expression of *HDAC7*, *PCDHB4*, and *HSPB3* in SCLC tumors and adjacent normal tissues. The differences between groups were analyzed by Wilcoxon test and $p < 0.05$ was considered statistically significant.

Furthermore, we validated the three genes (*HDAC7*, *PCDHB4*, and *HSPB3*) using an independent SCLC dataset (GEO: GSE60052). Kaplan-Meier analysis demonstrated that SCLC patients with higher *PCDHB4* expression or lower *HDAC7* expression exhibited worse OS. There was no significant difference in the OS between the SCLC patients with high and low *HSPB3* expression (Figure 3D).

In the George dataset, the expression of *PCDHB4* was significantly higher in late-stage SCLC tumors than in early-stage SCLC tumors, while the expression of *HDAC7* and *HSPB3* was not significantly different between late-stage and early-stage SCLC tumors (Figure 3E). We then examined the expression of *HDAC7*, *PCDHB4*, and *HSPB3* in SCLC tumors and normal tissues. In both the GEO: GSE60052 and GEO: GSE40275 datasets, the expression of *PCDHB4* was significantly higher, and the expression of *HDAC7* was significantly lower in SCLC tumors compared with adjacent normal tissues (Figure 3F). The expression of *HSPB3* is significantly lower in SCLC tumors in the GEO: GSE40275 dataset, but not in the GEO: GSE60052 dataset (Figure 3F). Therefore, in all tested datasets, the *PCDHB4* expression is higher in SCLC tumors, and its higher expression in tumors exhibits a worse prognosis in SCLC patients.

Hypomethylation of CpG sites in the *PCDHB4* gene correlates with its high expression and cisplatin resistance in small cell lung cancer

We further assessed whether *PCDHB4* gene expression correlated with DNA methylation in its promoter region. In the GDSC database, the expression of *PCDHB4* was significantly higher in cisplatin-resistant SCLC cell lines (Figure 4A). Among the 4 CpG sites (cg06048354, cg24918705, cg08626876, and cg07129523) in the *PCDHB4* promoter region, the methylation levels of the 3 CpG sites (cg06048354, cg24918705 and cg08626876) were significantly lower in cisplatin-resistant SCLC cells (Figure 4A). In 54 SCLC cell lines, the methylation levels of the 4 CpG sites were negatively correlated with the expression of *PCDHB4* (Figure 4A).

In 54 SCLC cell lines, the expression of *PCDHB4* significantly correlated with the IC50 of cisplatin (Figure 4B). In addition, the methylation levels of the 2 CpG sites (cg24918705 and cg07129523) were negatively correlated with the IC50 of cisplatin in SCLC cells (Figure 4B). Notably, we found that in SCLC patients treated with chemotherapy, the OS of patients with low *PCDHB4* expression was significantly longer, and the progression-free survival (PFS) of SCLC patients with high *PCDHB4* expression was significantly shorter (Figure 4C). Therefore, the hypomethylation of CpG sites in the *PCDHB4* gene correlates with its high expression and cisplatin resistance, and high expression of *PCDHB4* in SCLC patients who received chemotherapy is associated with fast disease progression.

Hypomethylation of the *PCDHB4* gene in small cell lung cancer was validated by Methylated DNA immuno-precipitation sequencing and bisulfite sequencing PCR

We further detected the methylation status of the *PCDHB4* gene in our collected SCLC clinical samples. First, we used MeDIP-seq to detect the whole genome methylation level in SCLC tumors and adjacent normal tissues. According to the cut-off of $p < 0.05$ and $|\log_{10}FC| \geq 1$, 179,468 (2.18%) differentially methylated sites were detected between SCLC tumors and adjacent normal tissues (Figures 5A and 5B). 83.56% (149,959/179,468) of these differentially methylated sites were hypomethylated. The 149,959 hypomethylated sites were located in different regions of genes, including the Exon (98.45%), 3'UTR (97.28%), 5'UTR (98.30%), Downstream (87.77%), Distal Intergenic (74.72%), Intron (81.09%) and Promoter (95.83%) (Figure 5C). To understand the biological functions of the identified differentially methylated genes, we performed GO annotation analysis. The result indicated that the differentially methylated genes were significantly enriched in the regulation of neurogenesis, regulation of neuron projection development, and neuron to neuron synapse (Figure 5D). GSEA indicated that genes were significantly enriched in small cell lung cancer and neurotrophin signaling pathways (Figure 5E).

We then examined the methylation level of *PCDHB4* with the promoter region between SCLC tumors and normal tissues. We found that the methylation level of the *PCDHB4* promoter was significantly lower in SCLC tumors, compared with normal tissues (Figure 5F). Furthermore, we mapped the differentially methylated sites to the 22 autosomal chromosomes and visualized the site locations across the chromosomes, and *PCDHB4* gene was located in the hypomethylation region of chromosome 5 (Figure 5G). As indicated in Figure 5H, the methylation level in the *PCDHB4* promoter region including the 4 CpG sites (cg06048354, cg24918705, cg08626876, and cg07129523) was lower in SCLC tumors than in adjacent normal tissues. Interestingly, by MeDIP-seq, we detected the methylation level of the *PCDHB4* gene of blood cfDNA in an SCLC patient who was treated with carboplatin and etoposide. We observed that the methylation level of cfDNA in the CpG sites was lower when the patient relapsed than before treatment. Finally, by BSP, the CpG site (cg24918705) was validated to be demethylated in SCLC tumor, compared with normal tissue (Figure 5I). Therefore, our results validate that the *PCDHB4* gene is lowly methylated in SCLC.

The expression of *PCDHB4* in small cell lung cancer is high, which promotes cellular proliferation and chemo-resistance

Next, we performed RT-PCR, Western blot, and IHC experiments to validate whether the expression of *PCDHB4* was higher in SCLC. The result of RT-PCR showed higher mRNA levels of *PCDHB4* in four SCLC cell lines compared with normal cells (BEAS-2B). Meanwhile, western blot showed that the protein expressions were also higher in SCLC cells (Figure 6A). To further verify the expression of *PCDHB4* in SCLC clinical samples, IHC staining demonstrated that *PCDHB4* expression was higher in SCLC tumor tissues compared to normal tissues (Figure 6B).

To further elucidate the function of *PCDHB4* in SCLC, *in vitro* functional experiments were conducted. *PCDHB4* overexpression plasmid was transfected in SBC2 SCLC cells (Figure 6C). Cell proliferation assay demonstrated that the cisplatin-induced cell death was reduced when SBC2 cells were transfected with *PCDHB4* overexpression plasmid, compared with empty vector transfection (Figure 6D). Furthermore, overexpression of *PCDHB4* enhanced cell proliferation (Figure 6E). Therefore, these data indicate that *PCDHB4* is highly expressed in SCLC, which promotes cellular proliferation and chemo-resistance.

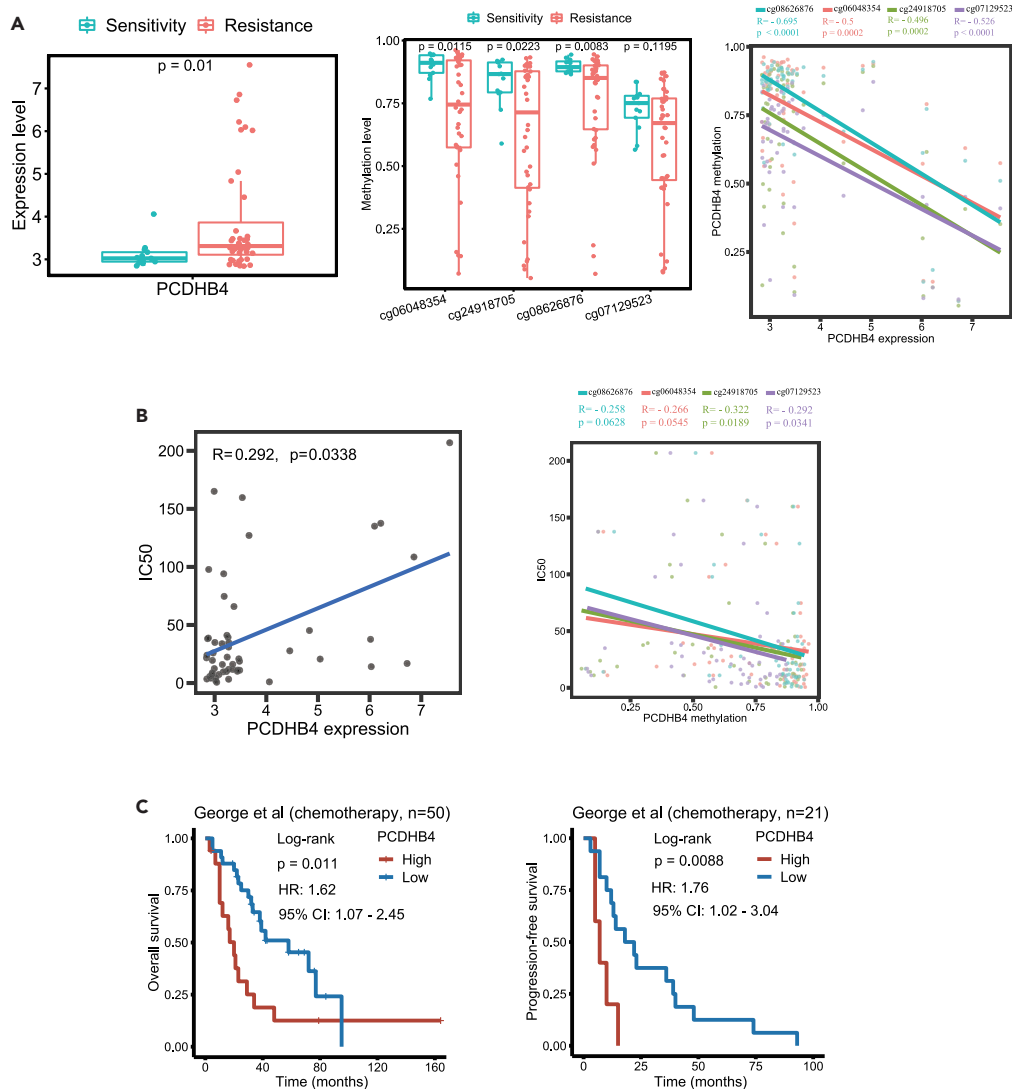


Figure 4. The correlation of *PCDHB4* methylation with its expression and cisplatin resistance in SCLC

(A) Boxplots showing *PCDHB4* expression (left panel) and methylation level of CpG sites within the *PCDHB4* promoter (middle panel) in cisplatin-sensitive and cisplatin-resistant SCLC cell lines. Correlation plot (right panel) showing the negative correlation between the CpG methylation level and the expression of *PCDHB4* in SCLC cell lines. The differences between groups were analyzed by Wilcoxon test and $p < 0.05$ was considered statistically significant.

(B) Correlation plot (left panel) showing the positive correlation between the *PCDHB4* expression and the cisplatin IC50 in SCLC cell lines. Correlation plot (right panel) showing the negative correlation between the *PCDHB4* CpG methylation level and the cisplatin IC50 in SCLC cell lines.

(C) Kaplan-Meier curves of SCLC patients treated with platinum-based chemotherapy using the George dataset.

Higher *PCDHB4* expression in small cell lung cancer tumors is associated with a lower infiltration level of immune cells

To explore the mechanism by which *PCDHB4* affects the prognosis of SCLC patients, functional analyses were used to identify potential biological processes and pathways enriched in SCLC tumors with high or low *PCDHB4* expression. In the George dataset, we identified the differentially expressed genes between the low and high *PCDHB4* expression groups. As indicated in the heatmap, 226 differentially expressed genes were identified (Figure 7A). Using the differentially expressed genes, the GO and KEGG analysis indicated significant enrichment of immune-associated signaling pathways, such as antigen processing and presentation, MHC protein complex, and natural killer cell-mediated cytotoxicity (Figures 7B and 7C). GSEA indicated that genes associated with low *PCDHB4* expression were significantly enriched in immune-related biological processes, such as antigen processing and presentation, B and T cell receptor signaling, and natural killer cell-mediated cytotoxicity (Figure 7D). Different algorithms, including TIMER, CIBERSORT, and XCELL, were used to evaluate immune cell infiltration in SCLC tumors (George cohort). The TIMER algorithm indicated that SCLC tumors with low *PCDHB4* expression had higher infiltration of B cells. The CIBERSORT and XCELL algorithms revealed that higher infiltration of T cells was present in SCLC tumors with low *PCDHB4*

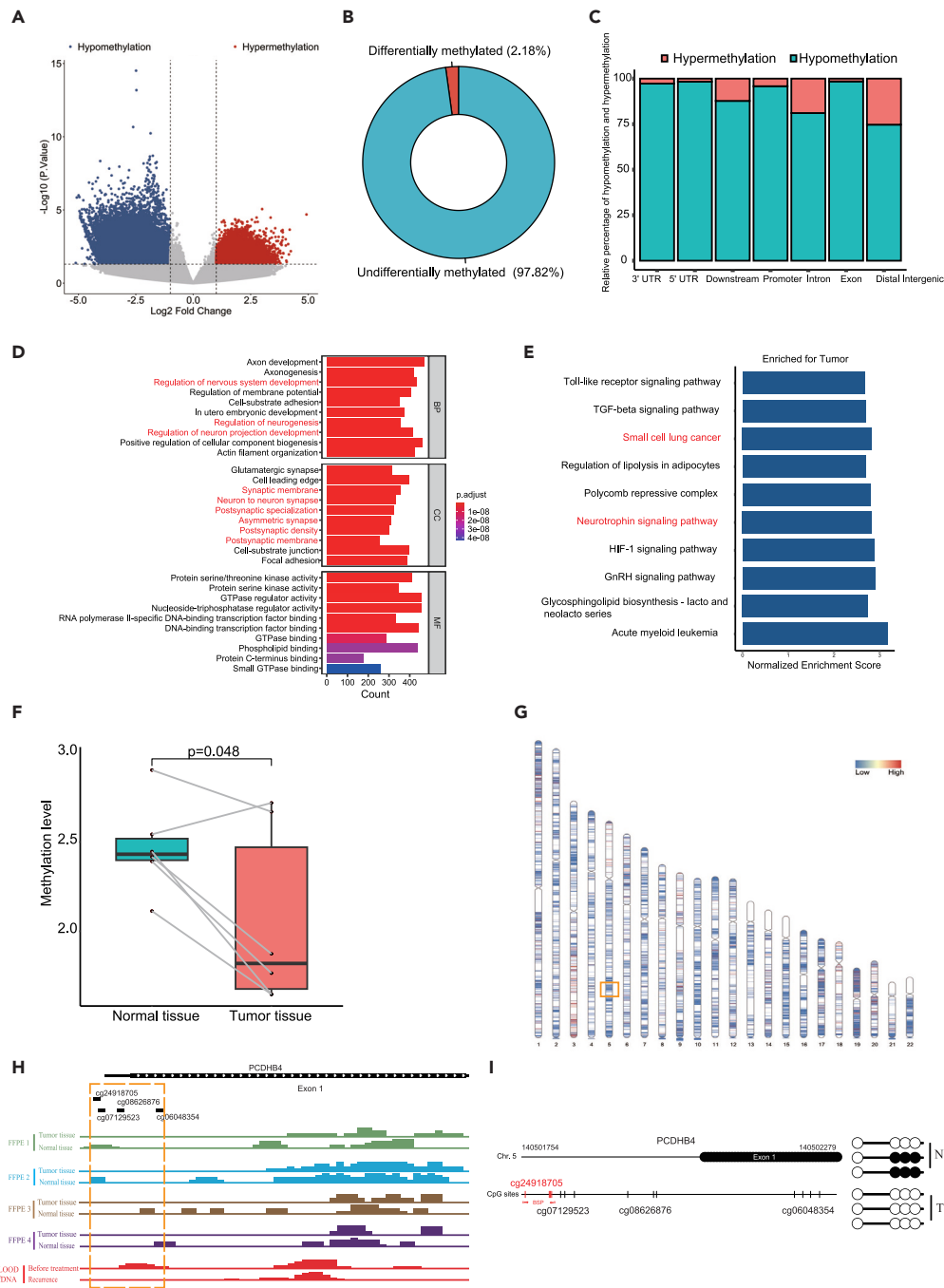


Figure 5. The validation of hypomethylation of the *PCDHB4* gene in SCLC specimens by MeDIP-seq and BSP

(A) Volcano plot of differentially methylated sites between SCLC tumors and adjacent normal tissues by MeDIP-seq.

(B) The proportion of differentially methylated sites in all detected methylated sites.

(C) The category of genomic locations for hypermethylated or hypomethylated sites.

(D) GO analysis for the differentially methylation genes. Top 10 terms are shown. Neuron-associated pathways are marked in red.

(E) Bar plot of GSEA based on the differentially methylation genes.

(F) Boxplot showing the methylation level within the *PCDHB4* promoter in SCLC tumors and adjacent normal tissues.

(G) Distribution of differentially methylated sites on chromosomes. The red area represents the hypermethylated region, and the blue area represents the hypomethylated region. The *PCDHB4* gene locates in the orange box.

(H) The peak maps of methylation with *PCDHB4* promoter by MeDIP-seq. DNA methylation was detected in SCLC tumors and adjacent normal tissues (FFPE 1, FFPE 2, FFPE 3, and FFPE 4) by MeDIP-seq. cfDNA methylation of an SCLC patient (before treatment and after recurrence) was detected by MeDIP-seq.

(I) BSP analysis of the CpG site cg24918705 in SCLC tumor and adjacent normal tissue.

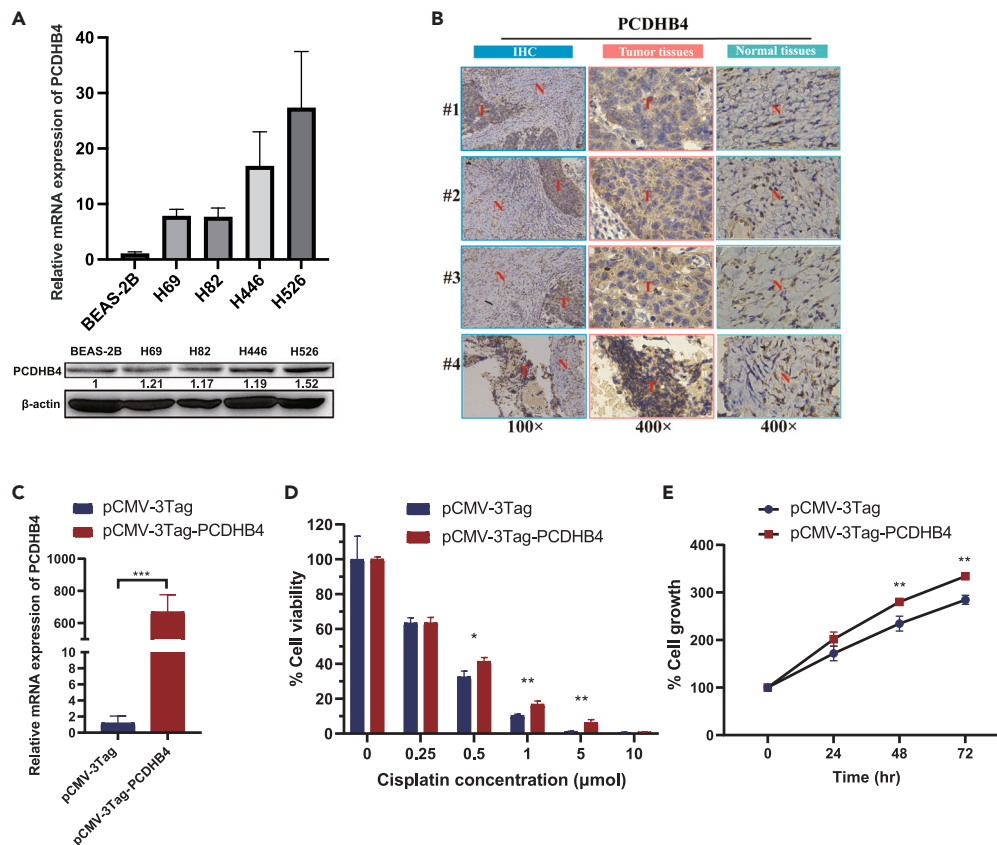


Figure 6. The expression of *PCDHB4* and *in vitro* functional analysis in SCLC

(A) qRT-PCR and western blot showing the higher expression of *PCDHB4* in SCLC cell lines (H69, H82, H446 and H526) compared with human lung epithelial cells (BEAS-2B).

(B) Representative IHC images of *PCDHB4* expression in SCLC clinical specimens. T: Tumor tissues, N: Normal tissues.

(C) *PCDHB4* overexpression in SBC2 cells confirmed by qRT-PCR. The differences between groups were analyzed by unpaired t-test (* $p < 0.05$, ** $p < 0.01$, *** $p < 0.001$).

(D) *PCDHB4* overexpression reduces the cell death of SBC2 cells induced by different concentrations of cisplatin. The differences between groups were analyzed by unpaired t-test (* $p < 0.05$, ** $p < 0.01$, *** $p < 0.001$).

(E) Cell proliferation assay of SBC2 cells transfected with control vector (pCMV-3Tag) and *PCDHB4* overexpression vector (pCMV-3Tag-PCDHB4). The differences between groups were analyzed by unpaired t-test (* $p < 0.05$, ** $p < 0.01$, *** $p < 0.001$).

expression (Figure 7E). The ssGSEA analysis showed that *PCDHB4* expression was negatively correlated with the content of memory B cells (Figure 7E). These data suggest that SCLC tumors with high *PCDHB4* expression exhibit low immune infiltration, which may lead to poor survival of SCLC patients.

Single-cell dissection of small cell lung cancer tumors with *PCDHB4* expression

Next, we included two scRNA-seq datasets (GEO: GSE138474 and publicly available dataset by Tian et al.¹³) to further dissect the expression characteristics of *PCDHB4* in SCLC tumors at single-cell resolution. In the GEO: GSE138474 dataset containing scRNA-seq data of SCLC CDXs,⁶ we screened out SCLC cells by neuroendocrine markers (*UCLH1*, *NCAM1*, *SYP*, and *CHGA*) and showed the dissimilarity and distribution of these cells by UMAP dimensionality reduction. We then dissected the *PCDHB4*-expressing cells at the single-cell level. In platinum-sensitive SCLC tumors (MDA-SC39 and MDA-SC4), *PCDHB4* was only expressed in 0.27% of SCLC cells. However, in platinum-resistant SCLC tumors (MDA-SC16 and MDA-SC49), *PCDHB4*-expressing cells were more abundant (3.77%) (Figure 8A). MDA-SC53 (vehicle) and MDA-SC53 (cisplatin) were SCLC CDXs (MDA-SC53) treated with vehicle control and cisplatin, until cisplatin-treated SCLC tumor relapsed. The UMAP plot showed that cisplatin-relapsed SCLC cells had a higher proportion of *PCDHB4*-expressing cells (5.66%) than vehicle-treated SCLC cells (4.96%) (Figure 8B). Furthermore, we found that both epithelial-mesenchymal transition (EMT) and stemness scores of SCLC cells were significantly higher in the platinum-resistant group, compared to the sensitive group (Figure 8C). We also assessed EMT and stemness scores in SCLC cells with *PCDHB4* expression and without *PCDHB4* expression. SCLC cells with *PCDHB4* expression had higher EMT and stemness scores, compared to SCLC cells without *PCDHB4* expression (Figure 8D).

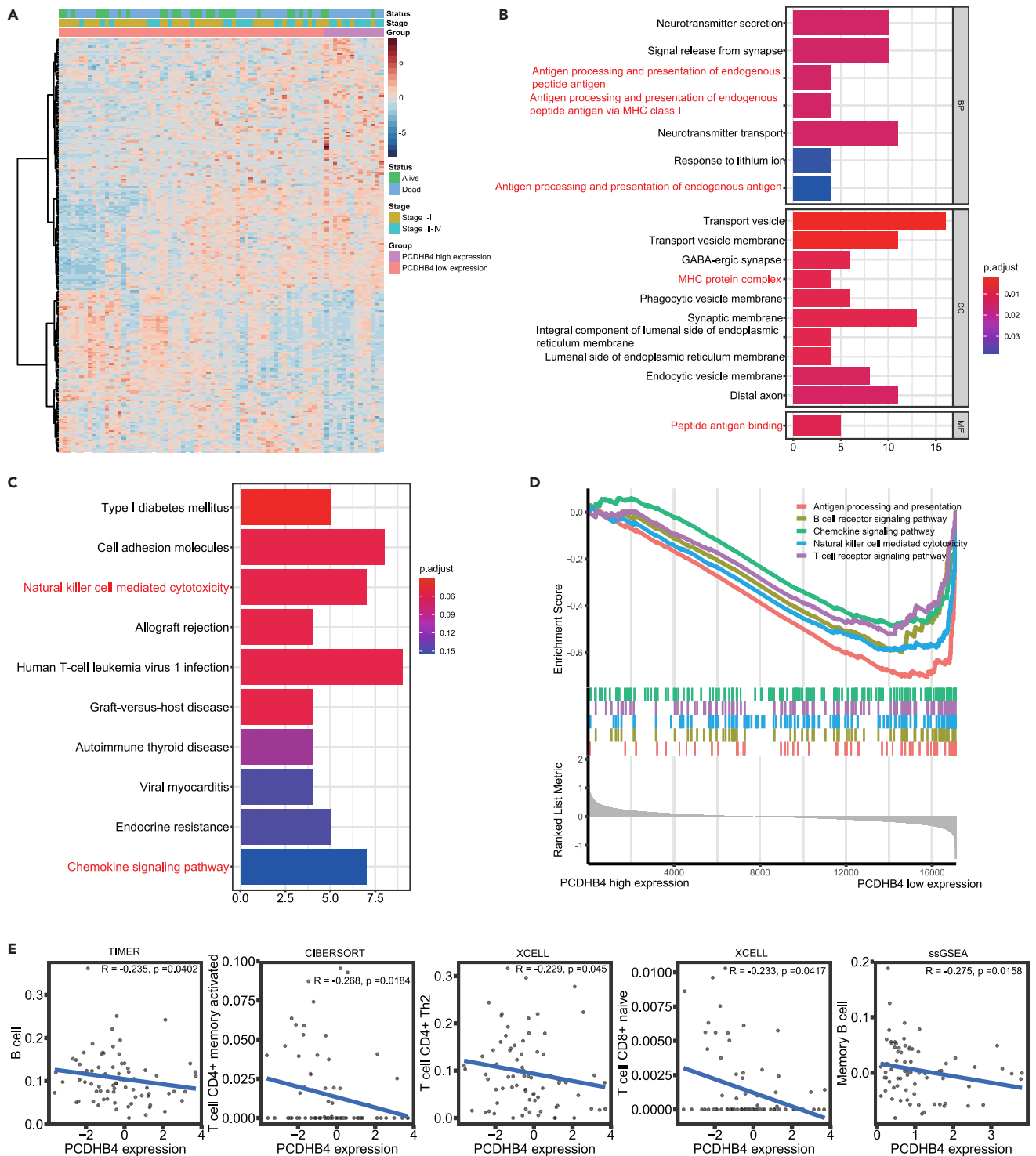


Figure 7. Functional enrichment analysis of SCLC tumors with low or high *PCDHB4* expression

(A) Heatmap of the differentially expressed genes between SCLC tumors with high and low *PCDHB4* expression.

(B) GO analysis for the differentially expressed genes. Immune-associated terms are marked in red.

(C) KEGG analysis for the differentially expressed genes. Immune-associated pathways are marked in red.

(D) GSEA between *PCDHB4*-high and *PCDHB4*-low expression group. Multiple immune-related gene sets are enriched in the *PCDHB4*-low expression group.

(E) The significant correlation of immune cell infiltration and *PCDHB4* expression in SCLC tumors obtained by different algorithms (TIMER, CIBERSORT, XCELL and ssGSEA).

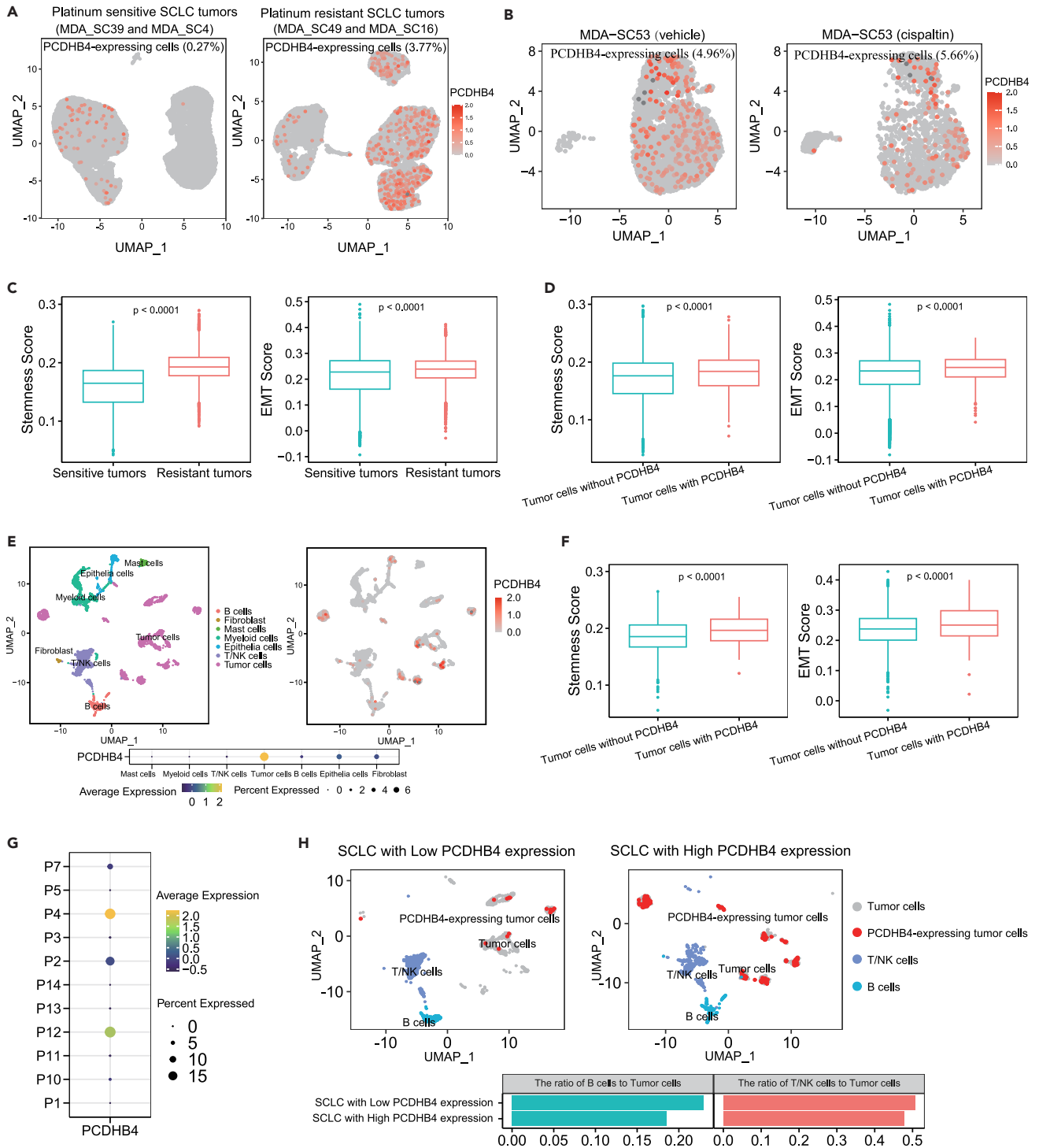


Figure 8. Single-cell dissection of SCLC tumors with *PCDHB4* expression

(A) UMAP plot of all SCLC tumor cells indicates the expression status of *PCDHB4* in platinum-sensitive and platinum-resistant SCLC tumors.
 (B) UMAP plot of all SCLC tumor cells indicates the expression status of *PCDHB4* in SCLC tumors receiving vehicle and cisplatin treatment.
 (C) Scoring of stemness and EMT gene signatures in platinum-sensitive and resistant SCLC tumors. The differences between groups were analyzed by Wilcoxon test and $p < 0.05$ was considered statistically significant.
 (D) Scoring of stemness and EMT gene signatures in SCLC cells with or without *PCDHB4* expression. The differences between groups were analyzed by Wilcoxon test and $p < 0.05$ was considered statistically significant.

Figure 8. Continued

- (E) UMAP plots indicate the clustering of all cell types and the expression of *PCDHB4* in all cell types. Bubble plot indicates that *PCDHB4* is predominantly expressed in tumor cells.
- (F) Scoring of stemness and EMT gene signatures in SCLC tumor cells with or without *PCDHB4* expression. The differences between groups were analyzed by Wilcoxon test and $p < 0.05$ was considered statistically significant.
- (G) Expression of *PCDHB4* in tumor cells of each SCLC patient. The SCLC patients (P2, P4, P7 and P12) are divided into the group with high *PCDHB4* expression. The SCLC patients (P1, P3, P5, P10, P11, P13, and P14) are divided into the group with low *PCDHB4* expression.
- (H) UMAP plot of all B cells, T/NK cells, and tumor cells indicates that the ratio of B cells or T/NK cells to tumor cells is higher in the group with low *PCDHB4* expression.

The dataset by Tian et al. contained scRNA-seq data of surgically resected SCLC tumors from 11 SCLC patients, including the single-cell transcriptome data of 7 distinct cell types (B cells, fibroblast, mast cells, myeloid cells, epithelial cells, T/NK cells, and tumor cells).¹³ The clustering of all cells revealed that *PCDHB4* was predominantly expressed in tumor cells (Figure 8E). Similarly, tumor cells expressing *PCDHB4* exhibited higher stemness and EMT scores, compared to tumor cells without *PCDHB4* expression (Figure 8F). Furthermore, according to the expression of *PCDHB4* in tumor cells, SCLC patients were divided into the group of SCLC with high *PCDHB4* expression (P2, P4, P7, and P12) and the group of SCLC with low *PCDHB4* expression (P1, P3, P5, P10, P11, P13, and P14) (Figure 8G). The clustering of T/NK cells, B cells, and tumor cells indicated that the ratio of T/NK cells or B cells to tumor cells was higher in the group with low *PCDHB4* expression, compared with the group with high *PCDHB4* expression (Figure 8H).

In summary, the single-cell sequencing data indicate that *PCDHB4*-expressing SCLC cells are associated with the “stemness” and “EMT” characteristics, as well as low immune infiltration.

Evaluation of *PCDHB4* as a prognostic marker in other subtypes of lung cancer

We further assessed whether the expression and CpG methylation of the *PCDHB4* gene were able to predict prognosis in other subtypes of lung cancer, lung adenocarcinoma (LUAD), and lung squamous cell carcinoma (LUSC). By mining TCGA data, shorter progression-free survival (PFS) and OS were observed in LUSC patients with higher *PCDHB4* expression (Figure 9A). In LUSC patients who had received platinum-based chemotherapy, we also found that the FPS was shorter in patients with higher *PCDHB4* expression (Figure 9B). According to the response to platinum-based chemotherapy, the LUSC patients were further divided into two groups: responders (patients who had a partial or complete response) and non-responders (patients who had clinical progressive or stable disease). As shown in Figure 9C, the expression of *PCDHB4* was significantly higher in the non-responder group.

In addition, shorter PFS and OS were also observed in LUSC patients with lower methylation levels of the CpG site (cg24918705) in the *PCDHB4* promoter (Figure 9D). Similarly, in LUSC patients receiving platinum-based chemotherapy, the PFS and OS of the patients with lower methylation levels of the CpG site (cg24918705) were shorter (Figure 9E). As shown in Figure 9F, in the non-responder group, the methylation level of the CpG site (cg24918705) was significantly lower.

However, we did not observe the correlation of the *PCDHB4* expression or CpG methylation with the survival in LUAD patients (data not shown). Therefore, the data suggest that the expression and CpG methylation (cg24918705) of the *PCDHB4* gene are prognostic markers in LUSC.

DISCUSSION

In this study, by integrating DNA methylation, gene expression, drug response, and clinical survival data, we found that the *PCDHB4* gene was poorly methylated and highly expressed in SCLC tumors, which was associated with the poor survival of SCLC patients.

PCDHB4 is a family member of protocadherin (PCDH) transmembrane proteins, which are predominantly expressed in the nervous system, and participate in cell-cell adhesion.¹⁴ Previous studies have demonstrated that PCDH expression is controlled by DNA methylation and its dysregulation is common in different types of cancer. Novak et al. reported DNA hypermethylation and transcriptional down-regulation of PCDH family genes in breast cancer.¹⁵ Dallosso et al. found DNA hypermethylation of the *PCDHA*, *PCDHB* and *PCDHG* genes in both adenomas and colorectal carcinomas. Particularly, *PCDHGC3* has been found to be highly methylated only in carcinomas and not in adenomas, thereby being proposed as a driver for the progression from adenoma to carcinoma.¹⁶ Abe et al. showed that the high methylation of *PCDHB16* was associated with poor survival in neuroblastoma.¹⁷

However, our study found that *PCDHB4* was hypomethylated and up-regulated in SCLC tumors. Some studies have demonstrated that hypomethylation and high expression of specific PCDHs correlated with cancer progression. Vega-Benedetti et al. indicated that hypomethylation of *PCDHGC5* correlated with its high expression in low-grade glioma (LGG), which was a poor survival predictive biomarker for LGG patients.¹⁸ *PCDH10* has been shown to be required for the proliferation and tumorigenicity of glioblastoma.¹⁹ Mukai et al. indicated that *PCDHB9* was over-expressed in gastric cancer, which correlated with poor survival.²⁰ Zhou et al. demonstrated that the over-expression of *PCDH7* was associated with poor clinical outcome in non-small cell lung cancer.²¹

The molecular mechanisms of PCDH proteins in cancer progression and drug resistance remain largely unknown. Previous studies have demonstrated that PCDH proteins regulate cancer cell proliferation and apoptosis via Wnt/ β -catenin, PI3K/AKT, and NF- κ B signalings.¹⁴ Our single-cell analysis found that *PCDHB4*-expressing SCLC cells exhibited more characteristics of stemness and EMT. Previous study has demonstrated that the activation of stemness and EMT program promotes the development of treatment resistance in cancer cells.²² A

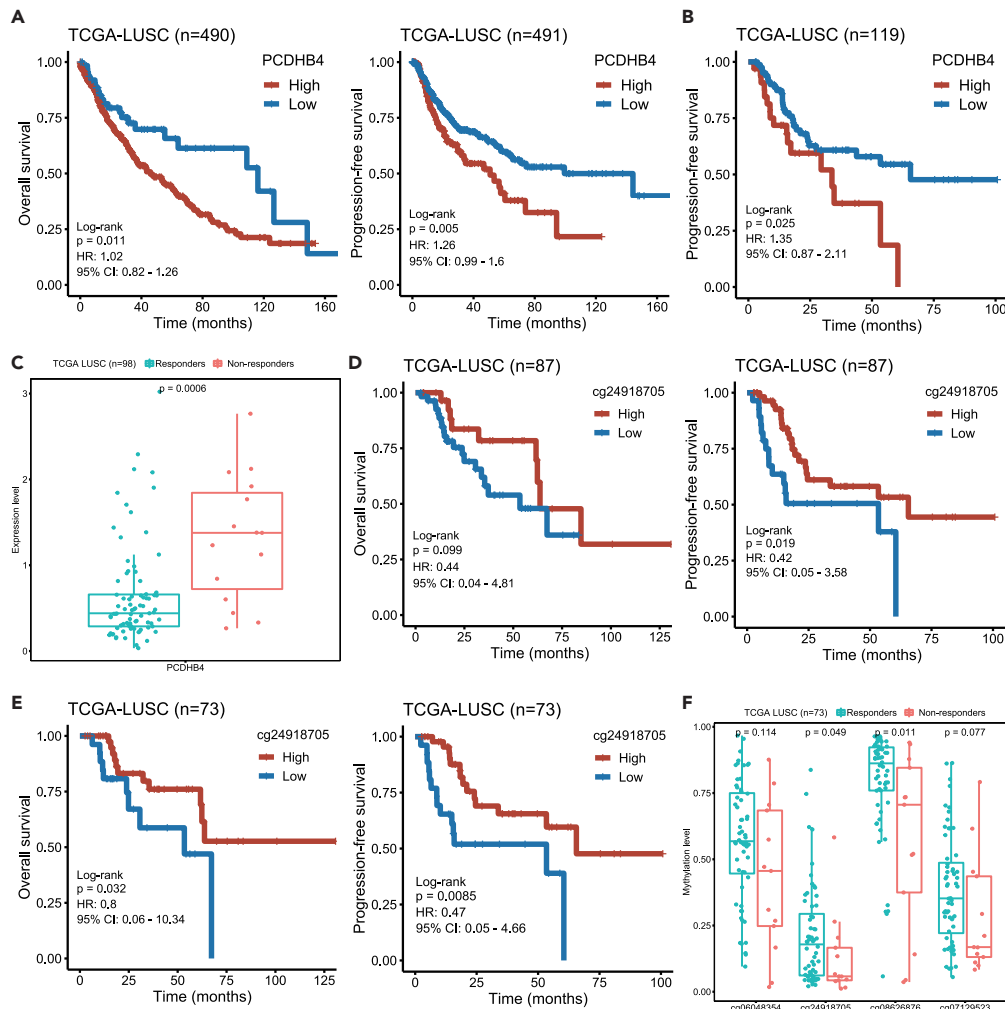


Figure 9. The expression and CpG methylation of the *PCDHB4* as prognostic markers in LUSC

(A) Kaplan-Meier curves of OS (left panel) and PFS (right panel) of LUSC patients with low and high *PCDHB4* expression.
 (B) Kaplan-Meier curves of the PFS of LUSC patients with low and high *PCDHB4* expression, who were treated with platinum-based chemotherapy.
 (C) Boxplot showing the expression of *PCDHB4* in LUSC patients who were responsive or non-responsive to platinum-based chemotherapy. The differences between groups were analyzed by Wilcoxon test and $p < 0.05$ was considered statistically significant.
 (D) Kaplan-Meier curves of OS (left panel) and PFS (right panel) of LUSC patients with low and high methylation levels of the *PCDHB4* CpG site (cg24918705).
 (E) Kaplan-Meier curves of OS (left panel) and PFS (right panel) of LUSC patients with low and high methylation levels of *PCDHB4* CpG site (cg24918705), who were treated with platinum-based chemotherapy.
 (F) Boxplot showing the methylation level of *PCDHB4* CpG sites in LUSC patients who were responsive or non-responsive to platinum-based chemotherapy. The differences between groups were analyzed by Wilcoxon test and $p < 0.05$ was considered statistically significant.

previous study indicated that the expression of *PCDHB* family genes was high in SCLC with high *SOX4* expression. The *SOX4* transcription factor was recruited to the promoter of *PCDHB* family genes to induce their expression.²³ Sox family proteins have been shown to play an important role in the maintenance of cancer stem cells.²⁴ A previous study reported that *SOX4* expression was up-regulated in glioblastoma and particularly high in malignant glioma initiating cells.²⁵ On the other hand, our study indicated that *PCDHB4*-expressing cells correlated with a low level of immune infiltration in SCLC tumors. Previous studies have indicated that protocadherin-18 (*PCDH18*) is an inhibitory signaling receptor that regulates tumor-infiltrating CD8⁺ memory T cells.²⁶ Therefore, our study suggests that *PCDHB4*-expressing SCLC cells exhibit the characteristics of stemness and EMT, which could lead to chemo-resistance and progression. Moreover, *PCDHB4*-expressing SCLC cells may have an inhibitory effect on tumor immune infiltration in SCLC.

In conclusion, the integrated analysis of DNA methylation and gene expression identified a novel prognostic marker, *PCDHB4*, in SCLC. The low CpG methylation and high expression of *PCDHB4* were also poor prognostic markers in LUSC. SCLC tumors with high *PCDHB4*

expression were characterized by the cancer stem cell phenotype and low immune infiltration. The *PCDHB4* gene as a potential prognostic biomarker warrants further investigation in large SCLC and LUSC clinical samples.

Limitations of the study

Although this study already performed multi-omics analyses combined with clinical data and the validation at different levels, there were still several limitations. Firstly, the prognostic value of *PCDHB4* expression and methylation needs be validated in a larger population of SCLC patients. Secondly, the detailed mechanism that *PCDHB4* expression leads to chemo-resistance and SCLC progression needs to be studied furtherly.

STAR★METHODS

Detailed methods are provided in the online version of this paper and include the following:

- KEY RESOURCES TABLE
- RESOURCE AVAILABILITY
 - Lead contact
 - Materials availability
 - Data and code availability
- EXPERIMENTAL MODEL AND STUDY PARTICIPANT DETAILS
 - Ethics approval and consent to participate
- METHOD DETAILS
 - Data collection
 - DNA extraction
 - Cell culture and *in vitro* functional experiment
 - Methylated DNA immuno-precipitation sequencing (MeDIP-seq) and data processing
 - Bisulfite sequencing PCR (BSP)
 - Real-time quantitative PCR (RT-PCR)
 - Western blot
 - Immunohistochemistry (IHC)
 - Functional enrichment and immune infiltration analyses
 - The process of scRNA-seq data analysis
- QUANTIFICATION AND STATISTICAL ANALYSIS

SUPPLEMENTAL INFORMATION

Supplemental information can be found online at <https://doi.org/10.1016/j.isci.2024.110413>.

ACKNOWLEDGMENTS

This study was supported by the National Natural Science Foundation of China (52072360 and 81872438), the Program of Research and Development of Key Common Technologies and Engineering of Major Scientific and Technological Achievements in Hefei (2021YL007), the Collaborative Innovation Program of Hefei Science Center, CAS (2022HSC-CIP015), and the Program of Clinical Medical Translational Research in Anhui Province (202304295107020092).

AUTHOR CONTRIBUTIONS

B.H. and W.X. designed the study. Q.Z., J.Q., and J.N. performed the bioinformatic analysis. M.F. and R.D. performed the MeDIP-seq, BSP, RT-PCR, Western blot, and IHC experiments. Z.X., D.W., J.L., X.W., and H.W. collected the SCLC clinical samples. Y.W. and Z.W. performed the *in vitro* functional experiments. Q.Z. and B.H. wrote the manuscript. All authors reviewed the manuscript.

DECLARATION OF INTERESTS

The authors have no financial/commercial conflicts of interest regarding the study.

Received: November 10, 2023

Revised: April 27, 2024

Accepted: June 26, 2024

Published: June 28, 2024

REFERENCES

- Gazdar, A.F., Bunn, P.A., and Minna, J.D. (2017). Small-cell lung cancer: what we know, what we need to know and the path forward. *Nat. Rev. Cancer* 17, 765.
- Oronsky, B., Reid, T.R., Oronsky, A., and Carter, C.A. (2017). What's New in SCLC? A Review. *Neoplasia* 19, 842–847.
- Sabari, J.K., Lok, B.H., Laird, J.H., Poirier, J.T., and Rudin, C.M. (2017). Unravelling the biology of SCLC: implications for therapy. *Nat. Rev. Clin. Oncol.* 14, 549–561.
- Rudin, C.M., Poirier, J.T., Byers, L.A., Dive, C., Dowlati, A., George, J., Heymach, J.V., Johnson, J.E., Lehman, J.M., MacPherson, D., et al. (2019). Molecular subtypes of small cell lung cancer: a synthesis of human and mouse model data. *Nat. Rev. Cancer* 19, 289–297.
- Gay, C.M., Stewart, C.A., Park, E.M., Diao, L., Groves, S.M., Heeke, S., Nabet, B.Y., Fujimoto, J., Solis, L.M., Lu, W., et al. (2021). Patterns of transcription factor programs and immune pathway activation define four major subtypes of SCLC with distinct therapeutic vulnerabilities. *Cancer Cell* 39, 346–360.e7.
- Stewart, C.A., Gay, C.M., Xi, Y., Sivajothi, S., Sivakamasundari, V., Fujimoto, J., Bolisetty, M., Hartsfield, P.M., Balasubramanian, V., Chalishazar, M.D., et al. (2020). Single-cell analyses reveal increased intratumoral heterogeneity after the onset of therapy resistance in small-cell lung cancer. *Nat. Cancer* 1, 423–436.
- Chan, J.M., Quintanal-Villalonga, Á., Gao, V.R., Xie, Y., Allaj, V., Chaudhary, O., Masilionis, I., Egger, J., Chow, A., Walle, T., et al. (2021). Signatures of plasticity, metastasis, and immunosuppression in an atlas of human small cell lung cancer. *Cancer Cell* 39, 1479–1496.e18.
- Gardner, E.E., Lok, B.H., Schneeberger, V.E., Desmeules, P., Miles, L.A., Arnold, P.K., Ni, A., Khodos, I., de Stanchina, E., Nguyen, T., et al. (2017). Chemosensitive Relapse in Small Cell Lung Cancer Proceeds through an EZH2-SLFN11 Axis. *Cancer Cell* 31, 286–299.
- Laird, P.W. (2003). The power and the promise of DNA methylation markers. *Nat. Rev. Cancer* 3, 253–266.
- Kalari, S., Jung, M., Kernstine, K.H., Takahashi, T., and Pfeifer, G.P. (2013). The DNA methylation landscape of small cell lung cancer suggests a differentiation defect of neuroendocrine cells. *Oncogene* 32, 3559–3568.
- Krushkal, J., Silvers, T., Reinhold, W.C., Sonkin, D., Vural, S., Connelly, J., Varna, S., Meltzer, P.S., Kunkel, M., Rapisarda, A., et al. (2020). Epigenome-wide DNA methylation analysis of small cell lung cancer cell lines suggests potential chemotherapy targets. *Clin. Epigenetics* 12, 93.
- George, J., Lim, J.S., Jang, S.J., Cun, Y., Ozretić, L., Kong, G., Leenders, F., Lu, X., Fernández-Cuesta, L., Bosco, G., et al. (2015). Comprehensive genomic profiles of small cell lung cancer. *Nature* 524, 47–53.
- Tian, Y., Li, Q., Yang, Z., Zhang, S., Xu, J., Wang, Z., Bai, H., Duan, J., Zheng, B., Li, W., et al. (2022). Single-cell transcriptomic profiling reveals the tumor heterogeneity of small-cell lung cancer. *Signal Transduct. Target. Ther.* 7, 346.
- Pancho, A., Aerts, T., Mitsogiannis, M.D., and Seuntjens, E. (2020). Protocadherins at the Crossroad of Signaling Pathways. *Front. Mol. Neurosci.* 13, 117.
- Novak, P., Jensen, T., Oshiro, M.M., Watts, G.S., Kim, C.J., and Futscher, B.W. (2008). Agglomerative epigenetic aberrations are a common event in human breast cancer. *Cancer Res.* 68, 8616–8625.
- Dallosso, A.R., Øster, B., Greenhough, A., Thorsen, K., Curry, T.J., Owen, C., Hancock, A.L., Szemes, M., Paraskeva, C., Frank, M., et al. (2012). Long-range epigenetic silencing of chromosome 5q31 protocadherins is involved in early and late stages of colorectal tumorigenesis through modulation of oncogenic pathways. *Oncogene* 31, 4409–4419.
- Abe, M., Ohira, M., Kaneda, A., Yagi, Y., Yamamoto, S., Kitano, Y., Takato, T., Nakagawara, A., and Ushijima, T. (2005). CpG island methylator phenotype is a strong determinant of poor prognosis in neuroblastomas. *Cancer Res.* 65, 828–834.
- Vega-Benedetti, A.F., Loi, E., Moi, L., Blois, S., Fadda, A., Antonelli, M., Arcella, A., Badiali, M., Giangaspero, F., Morra, I., et al. (2019). Clustered protocadherins methylation alterations in cancer. *Clin. Epigenetics* 11, 100.
- Echizen, K., Nakada, M., Hayashi, T., Sabit, H., Furuta, T., Nakai, M., Koyama-Nasu, R., Nishimura, Y., Taniue, K., Morishita, Y., et al. (2014). PCDH10 is required for the tumorigenicity of glioblastoma cells. *Biochem. Biophys. Res. Commun.* 444, 13–18.
- Mukai, S., Oue, N., Oshima, T., Imai, T., Sekino, Y., Honma, R., Sakamoto, N., Sentani, K., Kuniyasu, H., Egi, H., et al. (2017). Overexpression of PCDHB9 promotes peritoneal metastasis and correlates with poor prognosis in patients with gastric cancer. *J. Pathol.* 243, 100–110.
- Zhou, X., Updegraff, B.L., Guo, Y., Peyton, M., Girard, L., Larsen, J.E., Xie, X.J., Zhou, Y., Hwang, T.H., Xie, Y., et al. (2017). PROTOCADHERIN 7 Acts through SET and PP2A to Potentiate MAPK Signaling by EGFR and KRAS during Lung Tumorigenesis. *Cancer Res.* 77, 187–197.
- Shibue, T., and Weinberg, R.A. (2017). EMT, CSCs, and drug resistance: the mechanistic link and clinical implications. *Nat. Rev. Clin. Oncol.* 14, 611–629.
- Castillo, S.D., Matheu, A., Mariani, N., Carretero, J., Lopez-Rios, F., Lovell-Badge, R., and Sanchez-Cespedes, M. (2012). Novel transcriptional targets of the SRY-HMG box transcription factor SOX4 link its expression to the development of small cell lung cancer. *Cancer Res.* 72, 176–186.
- Pouremamali, F., Vahedian, V., Hassani, N., Mirzaei, S., Pouremamali, A., Kazemzadeh, H., Faridvand, Y., Jafari-Gharabaghlu, D., Nouri, M., and Maroufi, N.F. (2022). The role of SOX family in cancer stem cell maintenance: With a focus on SOX2. *Pathol. Res. Pract.* 231, 153783.
- Vervoort, S.J., van Boxtel, R., and Coffey, P.J. (2013). The role of SRY-related HMG box transcription factor 4 (SOX4) in tumorigenesis and metastasis: friend or foe? *Oncogene* 32, 3397–3409.
- Vazquez-Cintrón, E.J., Monu, N.R., Burns, J.C., Blum, R., Chen, G., Lopez, P., Ma, J., Radoja, S., and Frey, A.B. (2012). Protocadherin-18 is a novel differentiation marker and an inhibitory signaling receptor for CD8+ effector memory T cells. *PLoS One* 7, e36101.
- Yang, W., Soares, J., Greninger, P., Edelman, E.J., Lightfoot, H., Forbes, S., Bindal, N., Beare, D., Smith, J.A., Thompson, I.R., et al. (2013). Genomics of Drug Sensitivity in Cancer (GDSC): a resource for therapeutic biomarker discovery in cancer cells. *Nucleic Acids Res.* 41, D955–D961.
- Jiang, L., Huang, J., Higgs, B.W., Hu, Z., Xiao, Z., Yao, X., Conley, S., Zhong, H., Liu, Z., Brohawn, P., et al. (2016). Genomic Landscape Survey Identifies SRSF1 as a Key Oncodriver in Small Cell Lung Cancer. *PLoS Genet.* 12, e1005895.
- Qi, J., Hong, B., Tao, R., Sun, R., Zhang, H., Zhang, X., Ji, J., Wang, S., Liu, Y., Deng, Q., et al. (2021). Prediction model for malignant pulmonary nodules based on cfMeDIP-seq and machine learning. *Cancer Sci.* 112, 3918–3923.
- Boyer, L.A., Lee, T.I., Cole, M.F., Johnstone, S.E., Levine, S.S., Zucker, J.P., Guenther, M.G., Kumar, R.M., Murray, H.L., Jenner, R.G., et al. (2005). Core transcriptional regulatory circuitry in human embryonic stem cells. *Cell* 122, 947–956.
- Schliekelman, M.J., Taguchi, A., Zhu, J., Dai, X., Rodriguez, J., Celiktas, M., Zhang, Q., Chin, A., Wong, C.H., Wang, H., et al. (2015). Molecular portraits of epithelial, mesenchymal, and hybrid States in lung adenocarcinoma and their relevance to survival. *Cancer Res.* 75, 1789–1800.

STAR★METHODS

KEY RESOURCES TABLE

REAGENT or RESOURCE	SOURCE	IDENTIFIER
Antibodies		
Anti-PCDH4	ThermoFisher Scientific	Cat# PA5-120577; RRID: AB_2914149
Anti-β-actin antibody	TransGen Biotech	Cat# HC201; RRID: AB_2860007
Bacterial and virus strains		
DH5α	TOLOBIO	Cat# CC96102-02
pClone007 Simple Vector	TsingKe Biotech	Cat# TSV-007S
Biological samples		
FFPE samples of human SCLC and adjacent non-tumor tissues	The First Affiliated Hospital of USTC (Hefei, China)	N/A
Blood samples of SCLC patients	The First Affiliated Hospital of USTC (Hefei, China)	N/A
Chemicals, peptides, and recombinant proteins		
RPMI-1640	Gibco	Cat# 11875500BT
Fetal bovine serum	ExCell Bio	Cat# FSP500
Penicillin-streptomycin solution	Hyclone	Cat# SV30010
Cisplatin	MCE	Cat# HY-17394
Critical commercial assays		
GeneRead DNA FFPE Kit	Qiagen	Cat# 180134
Circulating Nucleic Acids Kit	Qiagen	Cat# 55114
DNA Methylation kit	Zymo Research	Cat# D5001
RNA extraction kit	Tiangen	Cat# DP451
Reverse transcription kit	TransGen	Cat# AT301-03
BCA Protein Assay Kit	Beyotime	Cat# P0009
NEBNext Multiplex Oligos for Illumina	New England BioLabs	Cat# E7335L
KAPA HiFi Hotstart ReadyMix	KAPA Biosystems	Cat# KK2602
KAPA HyperPrep Kit	KAPA Biosystems	Cat# KK8504
MagMeDIP Kit	Diagenode	Cat# C02010021
HighGene transfection reagent	ABclonal Technology	Cat# RM09014
CellTiter-Glo Luminescent Cell Viability assay	Promega	Cat# G7572
Deposited data		
Gene expression data and clinical information of SCLC	George et al. ¹²	https://doi.org/10.1038/nature14664
GEO: GSE60052	Gene Expression Omnibus (GEO) database	https://www.ncbi.nlm.nih.gov/geo/
GEO: GSE40275	Gene Expression Omnibus (GEO) database	https://www.ncbi.nlm.nih.gov/geo/
GEO: GSE138474	Gene Expression Omnibus (GEO) database	https://www.ncbi.nlm.nih.gov/geo/
SCLC scRNA-seq dataset	Tian et al. ¹³	https://doi.org/10.1038/s41392-022-01150-4
Gene expression data and clinical information of LUSC	TCGA	https://xenabrowser.net/datapages/
Genomics of Drug Sensitivity in Cancer (GDSC) database	GDSC	https://www.cancerrxgene.org/
MeDIP-seq data of SCLC	This study	GSA-Human: HRA007706

(Continued on next page)

Continued

REAGENT or RESOURCE	SOURCE	IDENTIFIER
<i>Experimental models: cell lines</i>		
BEAS-2B	Anhui Medical University	N/A
H69	ATCC	Cat# HTB-119
H82	ATCC	Cat# HTB-175
H446	Chinese Academy of Sciences	N/A
H526	ATCC	Cat# CRL-5811
SBC-2	HyCyte	Cat# TCH-C432
<i>Oligonucleotides</i>		
See Table S4 for primer sequence used in this study	This study	N/A
<i>Recombinant DNA</i>		
pCMV-3Tag	Agilent Technologies	Cat# 240195
pCMV-3Tag-PCDHB4	This study	N/A
<i>Software and algorithms</i>		
R	The R Project for Statistical Computing	www.r-project.org/
Survival	R CRAN	https://cran.r-project.org/web/packages/survival/index.html
survminer	R CRAN	https://cran.r-project.org/web/packages/survminer/index.html
limma	Bioconductor	https://bioconductor.org/packages/release/bioc/html/limma.html
ChAMP	Bioconductor	https://bioconductor.org/packages/release/bioc/html/ChAMP.html
clusterProfiler	Bioconductor	https://www.bioconductor.org/packages/release/bioc/html/clusterProfiler.html
Seurat	satijalab	https://satijalab.org/seurat/
GSVA	R package	https://github.com/rcastelo/GSVA
TIMER2.0	X Shirley Liu Lab 2020 Dana Farber Cancer Institute	http://timer.cistrome.org/
Macs2	Github	https://github.com/taoliu/MACS
deeptools	Github	https://github.com/deeptools/deepTools/
Integrative Genomics Viewer (IGV)	Broad Institute	https://software.broadinstitute.org/software/igv/
GraphPad Prism 9	GraphPad Software	https://www.graphpad.com/
ImageJ	ImageJ Software	https://imagej.nih.gov/ij

RESOURCE AVAILABILITY

Lead contact

Further information and requests for resources and reagents should be directed to and will be fulfilled by the lead contact, Bo Hong (bhong@hmf.ac.cn).

Materials availability

This study did not generate new unique reagents.

Data and code availability

- MeDIP-seq raw data of SCLC samples associated with this study have been deposited in the Genome Sequence Archive (GSA) in National Genomics Data Center, China National Center for Bioinformation/Beijing Institute of Genomics, Chinese Academy of Sciences (GSA-Human: HRA007706) that are publicly accessible at <https://ngdc.cncb.ac.cn/gsa-human>.

- This paper does not report the original code.
- Any additional information required to reanalyze the data reported in this paper is available from the [lead contact](#) upon request.

EXPERIMENTAL MODEL AND STUDY PARTICIPANT DETAILS

Ethics approval and consent to participate

This study was approved by the Clinical Research Ethics Committee of The First Affiliated Hospital of University of Science and Technology of China, with the approval number 2023-KY-136. SCLC clinical samples were obtained with written informed consent of the patients.

METHOD DETAILS

Data collection

We obtained the data on cisplatin IC50 values, gene expression and DNA CpG methylation of SCLC cell lines from the Genomics of Drug Sensitivity in Cancer (GDSC) database.²⁷ The gene expression of SCLC tumors and corresponding survival data were obtained from the datasets by George et al.¹² and GEO: GSE60052.²⁸ Among 77 SCLC patients in George dataset, 50 SCLC patients received chemotherapy. In GEO: GSE60052 dataset, all 48 SCLC patients received chemotherapy. The gene expression of SCLC tumors and adjacent normal tissues were obtained from GEO: GSE60052 and GEO: GSE40275. Two SCLC scRNA-seq datasets (GEO: GSE138474 and the dataset by Tian et al.¹³) were included in this study. The data of LUSC, including gene expression, CpG methylation and clinical information, were obtained from TCGA.

DNA extraction

For formalin-fixed and paraffin-embedded (FFPE) samples, genomic DNAs of SCLC tumors and paired normal tissues were extracted using the GeneRead DNA FFPE Kit (Qiagen, Hilden, Germany). For cell-free DNA (cfDNA) of blood samples, cfDNAs of SCLC patients were isolated from 3 to 4 mL of plasma using the Circulating Nucleic Acids Kit (Qiagen, Hilden, Germany).

Cell culture and *in vitro* functional experiment

SCLC cell lines H69, H82, H446, H526, SBC-2 and human lung epithelial cells (BEAS-2B) were cultured in RPMI-1640 medium (Gibco, Life Technologies, Carlsbad, CA, USA) containing 10% fetal bovine serum (ExCell Bio, Shanghai, China) and 1% penicillin and streptomycin (Hyclone, GE Healthcare Life Sciences, Logan, UT, USA) in a wet incubator with 37°C in a 5% CO₂ atmosphere.

The coding region of *PCDHB4* gene was cloned into pCMV-3Tag expression vector to construct *PCDHB4* expression vector (pCMV-3Tag-*PCDHB4*). SBC2 cells (3×10^5) were seeded onto 6-well plates and incubated for 24 h. Cells were then transfected with 1 μg *PCDHB4* expression vector and empty vector using HighGene (ABclonal Technology, Wuhan, China). Two days after transfection, one part of transfectants was collected for RT-PCR to check whether *PCDHB4* was over-expressed. Other part of transfectants was replated onto 96-well plate and was treated with different doses of cisplatin and vehicle control for 72 h, and then cell viability was measured by CellTiter-Glo Luminescent assay (Promega, WI, USA).

To detect the growth of SCLC cells overexpressing *PCDHB4*, transfected SBC2 cells were replated onto 96-well plate. After 1, 2 and 3 days, cell viability was measured by CellTiter-Glo Luminescent assay (Promega, WI, USA).

Methylated DNA immuno-precipitation sequencing (MeDIP-seq) and data processing

MeDIP-seq was performed using previously published methods.²⁹ In brief, DNA samples were first subjected to fragmentation, end repair, A-tailing and adaptor ligation. Then, methylated DNA was immunoprecipitated with a 5-mC monoclonal antibody. The immunoprecipitated methylated-DNA was sequenced on the Illumina Nova 6000 platform to generate 150-bp paired-end reads. The sequencing statistics for each sample were summarized in [Table S3](#). After sequencing, Macs2 was used to identify the methylation peaks. Reads per kilobase per million mapped reads (RPKM) was used to normalize the number of reads by deeptools and visualized using IGV tools.

Bisulfite sequencing PCR (BSP)

Genomic DNA was chemically modified with sodium bisulfite using the DNA Methylation kit (Zymo Research, CA, USA). Bisulfite-treated genomic DNA was amplified with BSP primers, specific for the cg24918705 site. Nested PCR was performed for 35 cycles with an annealing temperature of 55°C. The "outer" and "inner" primers were shown in [Table S4](#). The PCR products were cloned into the T-vector (TsingKe Biotech, Beijing, China). The colonies were randomly chosen for Sanger sequencing.

Real-time quantitative PCR (RT-PCR)

Total RNA from cells was extracted using total RNA extraction kit (Tiangen, Beijing, China) and first strand cDNA was synthesized with a reverse transcription kit (TransGen Biotech, Beijing, China). The primers were shown in [Table S4](#). The quantification of mRNA expression was obtained with the $2^{-\Delta\Delta C_t}$ method.

Western blot

Lysis buffer was used to extract cellular proteins, and BCA Protein Assay Kit (Beyotime, Shanghai, China) was used to quantify protein concentration. The same amount of protein was run for SDS-polyacrylamide gel electrophoresis. The primary antibody used was anti-*PCDHB4* (1:1000 dilution, PA5-120577, ThermoFisher Scientific, MA, USA). The β -actin (1:5000 dilution, HC201, TransGen Biotech, Beijing, China) was used as loading control. The density of the band was quantified by ImageJ (NIH, USA).

Immunohistochemistry (IHC)

Immunostaining of *PCDHB4* protein was performed using a rabbit polyclonal anti-*PCDHB4* antibody (1:400 dilution, PA5-120577, ThermoFisher Scientific, MA, USA). For the IHC assay, paraffin sections were incubated with primary antibody against *PCDHB4* at room temperature for 60 min, secondary antibody at 37°C for 30 min then stained with DAB and haematoxylin.

Functional enrichment and immune infiltration analyses

The clusterProfiler was used to determine Gene Ontology (GO) terms and Kyoto Encyclopedia of Genes and Genomes (KEGG) pathways. Gene set enrichment analysis (GSEA) was conducted to explore the underlying pathway variations between two groups.

We estimated immune infiltration using the CIBERSORT, TIMER and XCELL algorithms through the TIMER2 resource. We also evaluated immune cell infiltration in each sample using single-sample GSEA (ssGSEA) with the GSVA.

The process of scRNA-seq data analysis

The scRNA-seq expression matrix was processed with the Seurat. The gene expression data were log-normalized by the "NormalizeData" function. The top 2,000 highly variable genes were used to aggregate samples into a merged dataset and then scale. The main cell clusters were reduced and visualized using uniform manifold approximation and projection (UMAP). "FeaturePlot" was used to visualize gene expression. The scores of gene expression signatures were evaluated with the AddModuleScore function provided by the Seurat package. The stemness score was calculated with a geneset by Boyer et al.³⁰ and the EMT score was evaluated using a geneset by Schliekelman et al.³¹

QUANTIFICATION AND STATISTICAL ANALYSIS

Univariate Cox model was conducted to identify genes that were significantly correlated with the survival. Multivariate Cox analysis was conducted to identify genes that were independent prognostic factors. Kaplan-Meier analysis was conducted to evaluate the survival rate for each group using the "survimer" R package, and the patients were assigned into two groups according to the optimal cut-off value. Differentially expressed genes were analyzed by the limma package. Differentially methylated CpGs were analyzed by the ChAMP package. The differences between groups were analyzed by Wilcoxon test and $p < 0.05$ was considered statistically significant.